



**HAL**  
open science

## Longitudinal head-to-head comparison of 11C-PiB and 18F-florbetapir PET in a Phase 2/3 clinical trial of anti-amyloid- $\beta$ monoclonal antibodies in dominantly inherited Alzheimer's disease

Charles D Chen, Austin Mccullough, Brian Gordon, Nelly Joseph-Mathurin, Shaney Flores, Nicole S Mckay, Diana A Hobbs, Russ Hornbeck, Anne M Fagan, Carlos Cruchaga, et al.

### ► To cite this version:

Charles D Chen, Austin Mccullough, Brian Gordon, Nelly Joseph-Mathurin, Shaney Flores, et al.. Longitudinal head-to-head comparison of 11C-PiB and 18F-florbetapir PET in a Phase 2/3 clinical trial of anti-amyloid- $\beta$  monoclonal antibodies in dominantly inherited Alzheimer's disease. *European Journal of Nuclear Medicine and Molecular Imaging*, 2023, 50 (9), pp.2669-2682. 10.1007/s00259-023-06209-0 . hal-04504639

**HAL Id: hal-04504639**

**<https://hal.science/hal-04504639>**

Submitted on 14 Mar 2024

**HAL** is a multi-disciplinary open access archive for the deposit and dissemination of scientific research documents, whether they are published or not. The documents may come from teaching and research institutions in France or abroad, or from public or private research centers.

L'archive ouverte pluridisciplinaire **HAL**, est destinée au dépôt et à la diffusion de documents scientifiques de niveau recherche, publiés ou non, émanant des établissements d'enseignement et de recherche français ou étrangers, des laboratoires publics ou privés.



Published in final edited form as:

*Eur J Nucl Med Mol Imaging*. 2023 July ; 50(9): 2669–2682. doi:10.1007/s00259-023-06209-0.

## Longitudinal head-to-head comparison of $^{11}\text{C}$ -PiB and $^{18}\text{F}$ -florbetapir PET in a Phase 2/3 clinical trial of anti-amyloid- $\beta$ monoclonal antibodies in dominantly inherited Alzheimer disease

*A full list of authors and affiliations appears at the end of the article.*

### Abstract

**Purpose**—Pittsburgh Compound-B ( $^{11}\text{C}$ -PiB) and  $^{18}\text{F}$ -florbetapir are amyloid- $\beta$  (A $\beta$ ) positron emission tomography (PET) radiotracers that have been used as endpoints in Alzheimer disease (AD) clinical trials to evaluate the efficacy of anti-A $\beta$  monoclonal antibodies. However, comparing drug effects between and within trials may become complicated if different A $\beta$  radiotracers were used. To study the consequences of using different A $\beta$  radiotracers to measure A $\beta$  clearance, we performed a head-to-head comparison of  $^{11}\text{C}$ -PiB and  $^{18}\text{F}$ -florbetapir in a Phase 2/3 clinical trial of anti-A $\beta$  monoclonal antibodies.

**Methods**—Sixty-six mutation-positive participants enrolled in the gantenerumab and placebo arms of the first Dominantly Inherited Alzheimer Network Trials Unit clinical trial (DIAN-TU-001) underwent both  $^{11}\text{C}$ -PiB and  $^{18}\text{F}$ -florbetapir PET imaging at baseline and during at least one follow-up visit. For each PET scan, regional standardized uptake value ratios (SUVRs), regional Centiloids, a global cortical SUVR, and a global cortical Centiloid value were calculated. Longitudinal changes in SUVRs and Centiloids were estimated using linear mixed models. Differences in longitudinal change between PET radiotracers and between drug arms were estimated using paired and Welch two sample t-tests, respectively. Simulated clinical trials were conducted to evaluate the consequences of some research sites using  $^{11}\text{C}$ -PiB while other sites use  $^{18}\text{F}$ -florbetapir for A $\beta$  PET imaging.

---

**Corresponding author:** Tammie L.S. Benzinger, Washington University School of Medicine, 660 South Euclid, Campus Box 8225, St. Louis, Mo 63110, Telephone: (314) 362-1558, Fax: (314) 362-5297, benzinger@wustl.edu.

#### Author Contributions

All authors contributed to the study conception and design. Data analysis was performed by Charles D. Chen. The first draft of the manuscript was written by Charles D. Chen and all authors commented on previous versions of the manuscript. All authors read and approved the final manuscript.

Trial registration: [ClinicalTrials.gov NCT01760005](https://clinicaltrials.gov/ct2/show/study/NCT01760005). Registered 31 December 2012. Retrospectively registered.

#### Ethics approval

The study was conducted in accordance with the Declaration of Helsinki (version 7) and the International Conference on Harmonization and Good Clinical Practice guidelines. Protocols for the study have received prior approval by the local Institutional Review Board (IRB) or Ethics Committee of each DIAN site, and by the Washington University IRB for the Knight ADRC. The clinical trial registration number is [NCT01760005](https://clinicaltrials.gov/ct2/show/study/NCT01760005).

#### Consent to participate

Participants or their caregivers provided written informed consent.

#### Consent to publish

This manuscript does not contain the details, images, or video of any individual person.

**Results**—In the placebo arm, the absolute rate of longitudinal change measured by global cortical  $^{11}\text{C}$ -PiB SUVRs did not differ from that of global cortical  $^{18}\text{F}$ -florbetapir SUVRs. In the gantenerumab arm, global cortical  $^{11}\text{C}$ -PiB SUVRs decreased more rapidly than global cortical  $^{18}\text{F}$ -florbetapir SUVRs. Drug effects were statistically significant across both A $\beta$  radiotracers. In contrast, the rates of longitudinal change measured in global cortical Centiloids did not differ between A $\beta$  radiotracers in either the placebo or gantenerumab arms, and drug effects remained statistically significant. Regional analyses largely recapitulated these global cortical analyses. Across simulated clinical trials, type I error was higher in trials where both A $\beta$  radiotracers were used versus trials where only one A $\beta$  radiotracer was used. Power was lower in trials where  $^{18}\text{F}$ -florbetapir was primarily used versus trials where  $^{11}\text{C}$ -PiB was primarily used.

**Conclusion**—Gantenerumab treatment induces longitudinal changes in A $\beta$  PET, and the absolute rates of these longitudinal changes differ significantly between A $\beta$  radiotracers. These differences were not seen in the placebo arm, suggesting that A $\beta$ -clearing treatments may pose unique challenges when attempting to compare longitudinal results across different A $\beta$  radiotracers. Our results suggest converting A $\beta$  PET SUVR measurements to Centiloids (both globally and regionally) can harmonize these differences without losing sensitivity to drug effects. Nonetheless, until consensus is achieved on how to harmonize drug effects across radiotracers, and since using multiple radiotracers in the same trial may increase type I error, multi-site studies should consider potential variability due to different radiotracers when interpreting A $\beta$  PET biomarker data and, if feasible, use a single radiotracer for the best results.

## Keywords

Pittsburgh compound B;  $^{18}\text{F}$ -florbetapir; gantenerumab; dominantly inherited Alzheimer disease

## Introduction

The first two anti-amyloid- $\beta$  (A $\beta$ ) drug arms of the first Dominantly Inherited Alzheimer Network Trials Unit clinical trial (DIAN-TU-001) evaluated the effects of the anti-A $\beta$  monoclonal antibodies gantenerumab and solanezumab in participants with dominantly inherited Alzheimer disease (DIAD) (1). Initial findings from Pittsburgh Compound-B ( $^{11}\text{C}$ -PiB) positron emission tomography (PET) imaging indicated that participants in the gantenerumab arm demonstrated longitudinal reduction of cerebral A $\beta$  levels.

$^{11}\text{C}$ -PiB and  $^{18}\text{F}$ -florbetapir (i.e. Amyvid) are A $\beta$  PET radiotracers that have been used as primary and secondary endpoints in AD clinical trials to evaluate the efficacy of anti-A $\beta$  monoclonal antibodies.  $^{11}\text{C}$ -PiB has been used in prior trials of bapineuzumab (2) and ponezumab (3), and  $^{18}\text{F}$ -florbetapir has been used in prior trials of aducanumab (4), crenezumab (2), donanemab (5), gantenerumab (6), lecanemab (7), and solanezumab (8) (Table 1).

However, comparing drug effects between trials may not be straightforward if different A $\beta$  radiotracers were used across trials. While  $^{11}\text{C}$ -PiB and  $^{18}\text{F}$ -florbetapir share numerous similarities, such as correlated binding characteristics (9) and shared high-affinity binding sites (10), they also demonstrate important differences, such as the greater white matter signal variability of  $^{18}\text{F}$ -florbetapir (9,11–13), and the lower cortical uptake relative to white

matter uptake of  $^{18}\text{F}$ -florbetapir, which has been hypothesized to contribute to the smaller range of standardized uptake value ratios (SUVRs) seen in  $^{18}\text{F}$ -florbetapir versus  $^{11}\text{C}$ -PiB PET (9). Whether the differences between  $^{11}\text{C}$ -PiB and  $^{18}\text{F}$ -florbetapir are enough to impact the interpretation of drug effects is unknown, as all prior work comparing the two A $\beta$  radiotracers were observational studies. Whether converting  $^{11}\text{C}$ -PiB and  $^{18}\text{F}$ -florbetapir SUVR results to the Centiloid scale (14) – as is often done in observational studies to standardize results from different A $\beta$  radiotracers to a common unit of measurement – will sufficiently harmonize  $^{11}\text{C}$ -PiB and  $^{18}\text{F}$ -florbetapir estimates of drug treatment is also unknown.

Among interventional studies, the DIAN-TU-001 is unique, as most participants underwent both  $^{11}\text{C}$ -PiB and  $^{18}\text{F}$ -florbetapir PET imaging at baseline and during at least one follow-up visit. This provides an opportunity to perform a head-to-head comparison of  $^{11}\text{C}$ -PiB and  $^{18}\text{F}$ -florbetapir to study the consequences of using different A $\beta$  radiotracers to measure A $\beta$  change in the same individuals.

## Materials and methods

### Study approval

The study was conducted in accordance with the Declaration of Helsinki (version 7) and the International Conference on Harmonization and Good Clinical Practice guidelines. Protocols for the study have received prior approval by the local Institutional Review Board (IRB) or Ethics Committee of each DIAN site, and by the Washington University IRB for the Knight ADRC. Participants or their caregivers provided written informed consent. The clinical trial registration number is [NCT01760005](https://clinicaltrials.gov/ct2/show/study/NCT01760005).

### Participant characteristics

In the DIAN-TU-001, 52 DIAD mutation-positive participants were enrolled in the gantenerumab arm and 40 DIAD mutation-positive participants were enrolled in the placebo arm (Supplemental figure 1). Among them, 41 participants in the gantenerumab arm and 25 participants in the placebo arm underwent both  $^{11}\text{C}$ -PiB and  $^{18}\text{F}$ -florbetapir PET imaging at baseline and during at least one follow-up visit (Table 2). During these visits,  $^{11}\text{C}$ -PiB and  $^{18}\text{F}$ -florbetapir PET were acquired with at most 28 days between imaging sessions.

Due to the lack of a significant effect on  $^{11}\text{C}$ -PiB PET outcomes in the solanezumab arm (1), the current study is limited to the gantenerumab and placebo arms.

### A $\beta$ PET acquisition

Participants were scanned on DIAN-approved PET scanners (15,16). Participants received a single  $13\pm 3$  (mean $\pm$ standard deviation) mCi intravenous bolus injection of  $^{11}\text{C}$ -PiB or a single  $9.8\pm 0.7$  (mean $\pm$ standard deviation) mCi intravenous bolus injection of  $^{18}\text{F}$ -florbetapir (Avid Radiopharmaceuticals, a wholly owned subsidiary of Eli Lilly and Company) at each imaging session. Emission data were collected 40–70 minutes post injection for  $^{11}\text{C}$ -PiB (17) and 50–70 minutes post injection for  $^{18}\text{F}$ -florbetapir (11). List-mode data were reconstructed using ordered subset expectation maximization. A low-dose CT scan preceded

PET acquisition for attenuation correction. Reconstructed PET images were processed using the PET Unified Pipeline (<https://github.com/ysu001/PUP>) (18,19). After segmenting MR images into regions of interest using FreeSurfer version 5.3 (20), regional standardized value uptake ratios (SUVRs) were defined from the reconstructed PET images using a cerebellar gray reference region. A global cortical SUVR for each image was defined as the sum of the mean bilateral SUVRs of the precuneus, superior frontal, rostral middle frontal, lateral orbitofrontal, medial orbitofrontal, superior temporal, and middle temporal ROIs. A global cortical Centiloid for each image was defined by standardizing the mean cortical SUVR to the Centiloid scale (11,14). Additionally, regional Centiloids were defined by standardizing regional SUVRs to the Centiloid scale by the direct conversion process (method-2) described in Klunk et al. (14).

### **MRI acquisition**

Participants were scanned on DIAN-approved 3T MRI scanners (15,16). Across all scanners, T1-weighted head MR images were acquired using magnetization prepared rapid gradient echo generalized autocalibrating partial parallel acquisition sequence with a repetition time=2300 ms, echo time=2.95 ms, flip angle=9°, and voxel resolution=1.1×1.1×1.2 mm<sup>3</sup>.

### **Statistical analysis of DIAN-TU-001 data**

Longitudinal annualized change in regional SUVRs, global cortical SUVRs, regional Centiloids, and global cortical Centiloids were estimated using linear mixed models. Linear mixed models included individual-level random intercepts and random slopes to account for the correlation across repeated measurements from the same individual over time. Differences in longitudinal change between PET radiotracers and between drug arms were estimated using paired and Welch two sample t-tests, respectively. In particular, test statistics pertaining to regional SUVRs had their p-values adjusted for false discovery rate (FDR) control by the Benjamini-Hochberg procedure (21) at the 0.05 level for discussion purposes.

All analyses were conducted using R version 4.0.2 (22).

### **Statistical simulations**

International clinical trials may necessitate the use of different A $\beta$  radiotracers within the same trial due to the availability of each radiotracer at each site. An analysis of each radiotracer separately may underpower the study, or it may lead to difficulties in interpretation if the cohorts receiving different radiotracers have differences in their demographics. Taking imaging measures derived from different radiotracers, harmonizing them by the Centiloid method, and then analyzing together would obtain an estimate of treatment efficacy. However, whether this harmonization is appropriate for treatment efficacy inference, e.g. control of type I error, influence on power, has not been investigated before. To evaluate the impact of allowing the use of multiple A $\beta$  PET radiotracers in the same trial, clinical trials were simulated such that participants were scanned with either <sup>11</sup>C-PiB or <sup>18</sup>F-florbetapir. Details of the simulations are as follows:

- Bivariate linear mixed models were fit to Centiloid-<sup>11</sup>C-PiB and Centiloid-<sup>18</sup>F-florbetapir data from the gantenerumab and placebo arms to obtain, for both radiotracers, simultaneously: (1) the covariance matrix of the random intercepts and slopes of the longitudinal data of these two radiotracers; (2) the within-subject error variance for each radiotracers; and (3) the baseline and slopes of each trial arm for each radiotracer.
- The parameters obtained above were then used to simulate individual-level longitudinal data for each radiotracer.
- The following conditions were simulated: sample size=20 participants per arm (treatment arm and placebo arm), 32 participants per arm, and 40 participants per arm; randomization ratio=1:1; participant dropout=0% annually and 5% annually; percentage of participants scanned with <sup>18</sup>F-florbetapir=100% (no participants scanned with <sup>11</sup>C-PiB), 75%, 50%, 25%, and 0% (all participants scanned with <sup>11</sup>C-PiB). For example, for sample size=20 participants per arm and <sup>18</sup>F-florbetapir=100%, all participant data in both the treatment and placebo arms were simulated based on the parameters estimated from the Centiloid-<sup>18</sup>F-florbetapir data, whereas for the same sample size and <sup>18</sup>F-florbetapir=75%, 15 participants of the 20 in each arm were simulated based on the parameters estimated from the Centiloid-<sup>18</sup>F-florbetapir data and 5 participants were simulated based on the parameters estimated from the Centiloid-<sup>11</sup>C-PiB data. These simulations aimed to cover a broad range of possible data mixing from both radiotracers to evaluate the impact of using two radiotracers on trial outcome in terms of type I error and power.
- Two scenarios were investigated: (1) The no treatment effect, namely both the treatment arm and the placebo arm were simulated using the parameters estimated from the placebo arm of the DIAN-TU-001 study. This provides an estimate of type I error; and (2) the observed treatment effect in the DIAN-TU-001 study, namely the treatment arm was simulated based on the parameters estimated from the gantenerumab arm of the DIAN-TU-001 study and the placebo arm was simulated based on the parameters estimated from the placebo arm of the DIAN-TU-001 study.
- Mimicking the DIAN-TU-001 study schedule (1), longitudinal data were simulated for each participant. Specifically, each participant's intercept and slope were first simulated based on parameters estimated from the trial, then each individual's longitudinal data were simulated using the intercept and slope plus a within-subject error term.
- Each simulated trial was analyzed using linear mixed models with random intercepts and slopes to estimate the difference in the slope (annualized rate of change) between the simulated treatment and simulated placebo arms and output a corresponding p-value. If the two-sided p-value was less than 0.05, then the corresponding trial was considered to reach statistical significance for treatment efficacy.

- A thousand simulated clinical trials were conducted for each scenario above. Overall power and type I error were calculated as the percentage of the 1000 simulated clinical trials that reached statistical significance at a two-sided type I error of 5%.

All simulations were conducted using SAS software, version 9.4.

## Results

### DIAN-TU-001 clinical trial results

Mean baseline global cortical SUVRs and Centiloids in the gantenerumab and placebo arms are shown in Table 3. The mean of baseline global cortical SUVRs calculated from  $^{11}\text{C}$ -PiB (global cortical SUVR- $^{11}\text{C}$ -PiB) in the gantenerumab arm (1.7, standard error [SE]=0.08 [4.8% of the mean]) was similar to that of the placebo arm (1.7, SE=0.09 [5.4%]), with no statistically significant difference (Welch two sample t-test p-value=0.74, Table 3). The mean of baseline global cortical SUVRs calculated from  $^{18}\text{F}$ -florbetapir (global cortical SUVR- $^{18}\text{F}$ -florbetapir) in the gantenerumab arm (1.5, SE=0.06 [3.7%]) was also similar to that of the placebo arm (1.4, SE=0.05 [3.7%]), with no statistically significant difference (Welch two sample t-test p-value=0.48, Table 3). Consistent with the higher dynamic range of  $^{11}\text{C}$ -PiB, mean baseline global cortical SUVR- $^{11}\text{C}$ -PiB and SUVR- $^{18}\text{F}$ -florbetapir showed statistically significant differences within the gantenerumab arm (paired t-test p-value= $2.7 \times 10^{-6}$ ) and within the placebo arm (paired t-test p-value=0.00030, Table 3).

The mean of baseline global cortical Centiloids calculated from  $^{11}\text{C}$ -PiB (global cortical Centiloid- $^{11}\text{C}$ -PiB) in the gantenerumab arm (63) was similar to that of the placebo arm (59), with no statistically significant difference (because the Centiloid process involves only a simple linear transformation, all Welch two sample t-test t- and p-values are the same across corresponding global cortical SUVR and global cortical Centiloid comparisons and will not be mentioned further). Likewise, the mean of baseline global cortical Centiloids calculated from  $^{18}\text{F}$ -florbetapir (global cortical Centiloid- $^{18}\text{F}$ -florbetapir) in the gantenerumab arm (61) was similar to that of the placebo arm (52). However, in contrast to global cortical SUVRs, baseline global cortical Centiloids calculated from the two A $\beta$  radiotracers did not show statistically significant differences within the gantenerumab arm (paired t-test p-value=0.67) or within the placebo arm (paired t-test p-value=0.25, Table 3).

Mean rate of longitudinal change in global cortical SUVRs and Centiloids in the gantenerumab and placebo arms are shown in Table 4. The mean annualized rate of global cortical SUVR- $^{11}\text{C}$ -PiB change in the gantenerumab arm ( $-0.045$  [ $-2.6\%$  change from baseline], SE=0.0086 [19% of the change]) differed from that of the placebo arm (0.022 [1.3%], SE=0.0081 [37%]) and this difference was statistically significant (Welch two sample t-test p-value= $6.6 \times 10^{-12}$ , Table 4 and Figure 4). The mean annualized rate of global cortical SUVR- $^{18}\text{F}$ -florbetapir change in the gantenerumab arm ( $-0.030$  [ $-2.0\%$ ], SE=0.0078 [26%]) differed from that of the placebo arm (0.015 [1.1%], SE=0.0088 [59%]) and this difference was statistically significant (Welch two sample t-test p-value= $1.7 \times 10^{-8}$ ). Comparing mean annualized rates of global cortical SUVR- $^{11}\text{C}$ -PiB and SUVR- $^{18}\text{F}$ -

florbetapir change within the gantenerumab arm showed statistically significant differences (paired t-test p-value=0.00034), but not within the placebo arm (paired t-test p-value=0.26, Table 4 and Figure 4).

Mean annualized rate of Centiloid-<sup>11</sup>C-PiB change in the gantenerumab arm (-4.6) differed from that of the placebo arm (2.2) and this difference was statistically significant. Likewise, the mean annualized rate of Centiloid-<sup>18</sup>F-florbetapir change in the gantenerumab arm (-4.9) differed from that of the placebo arm (2.5) and this difference was statistically significant. However, in contrast to global cortical SUVRs, annualized rates of global cortical Centiloid change calculated from the two A $\beta$  radiotracers did not show statistically significant differences within either the gantenerumab arm (paired t-test p-value=0.54) or within the placebo arm (paired t-test p-value=0.71, Table 4 and Figure 4).

Rates of longitudinal change in regional SUVRs are shown in Figure 1. Annualized rates of regional SUVR-<sup>11</sup>C-PiB and regional SUVR-<sup>18</sup>F-florbetapir change showed decreasing values across most brain areas in the gantenerumab arm (Figures 1A and 1B). In contrast, annualized rates of regional SUVR-<sup>11</sup>C-PiB and regional SUVR-<sup>18</sup>F-florbetapir change showed increasing values across most brain areas in the placebo arm (Figures 1C and 1D). Drug effects were statistically significant across all regional SUVR-<sup>11</sup>C-PiB and regional SUVR-<sup>18</sup>F-florbetapir results (Figures 1E and 1F).

Rates of longitudinal change in regional Centiloids are shown in Figure 2. Reporting longitudinal change in regional Centiloids recapitulated the above results: annualized rates of regional Centiloid-<sup>11</sup>C-PiB and regional Centiloid-<sup>18</sup>F-florbetapir change showed decreasing values across most brain areas in the gantenerumab arm (Figures 2A and 2B), increasing values across most brain areas in the placebo arm (Figures 2C and 2D), and drug effects remained statistically significant across all regional Centiloid-<sup>11</sup>C-PiB and regional Centiloid-<sup>18</sup>F-florbetapir results (Figures 2E and 2F).

However, while statistically significantly greater decreases in SUVR-<sup>11</sup>C-PiB versus SUVR-<sup>18</sup>F-florbetapir were observed across nearly every brain area in the gantenerumab arm, excepting the lateral orbitofrontal frontal gyrus, and basal regions of the temporal lobe and occipital lobe (Figure 3A), no statistically significantly different rates of change were seen in Centiloid-<sup>11</sup>C-PiB versus Centiloid-<sup>18</sup>F-florbetapir across most brain areas, excepting the lingual, parahippocampal, and entorhinal cortices (Centiloid-<sup>18</sup>F-florbetapir change greater than Centiloid-<sup>11</sup>C-PiB change), and most subcortical structures (Centiloid-<sup>11</sup>C-PiB change greater than Centiloid-<sup>18</sup>F-florbetapir) (Figure 3B). Similarly, while statistically significantly greater increases in SUVR-<sup>11</sup>C-PiB versus SUVR-<sup>18</sup>F-florbetapir were observed across several brain areas, including the medial orbitofrontal gyrus, and regions within the temporal lobe and medial occipital lobe (Figure 3A), no statistically significantly different rates of change in Centiloid-<sup>11</sup>C-PiB versus Centiloid-<sup>18</sup>F-florbetapir were found across most brain areas, excepting the amygdala (Figure 3B).

In addition, the difference between Centiloid-<sup>11</sup>C-PiB values at baseline for subcortical structures, for example, the caudate and putamen, versus the global cortical Centiloid-<sup>11</sup>C-PiB (mean caudate-global cortical Centiloid-<sup>11</sup>C-PiB=13, SE=4.7, 95% CI=[4.2, 23],



mean putamen-global cortical Centiloid-<sup>11</sup>C-PiB=38, SE=4.5, 95% CI=[29, 47]), is much larger than the difference between Centiloid-<sup>18</sup>F-florbetapir for those structures and the global cortical Centiloid-<sup>18</sup>F-florbetapir (mean caudate-global cortical Centiloid-<sup>18</sup>F-florbetapir=-3.3, SE=4.3, 95% CI=[-11, 5.1], mean putamen-global cortical Centiloid-<sup>18</sup>F-florbetapir=25, SE=3.7, 95% CI=[18, 32]), which is statistically significant (caudate-global cortical Centiloid-<sup>11</sup>C-PiB versus caudate-global cortical Centiloid-<sup>18</sup>F-florbetapir t-value=5.9, p-value=1.3×10<sup>-7</sup>, putamen-global cortical Centiloid-<sup>11</sup>C-PiB versus putamen-global cortical Centiloid-<sup>18</sup>F-florbetapir t-value=5.0, p-value=4.0×10<sup>-6</sup>).

### Simulated clinical trial results

The results of the simulated clinical trials where some participants are scanned with <sup>11</sup>C-PiB while others are scanned with <sup>18</sup>F-florbetapir are presented in Table 5. Under the no treatment effect scenario, type I error remained consistent across different sample sizes (20 participants per arm, 32 participants per arm, and 40 participants per arm), and increased as the proportion of participants scanned with the two radiotracers approached 50% each. Under the observed treatment effect scenario, power increased as sample size increased, and increased as the proportion of participants scanned with <sup>11</sup>C-PiB approached 100%. Finally, simulating a 5% annual dropout rate in the above scenarios tended to decrease power, but did not have a consistent effect on type I error.

### Discussion

Similarities and differences between the two Aβ radiotracers <sup>11</sup>C-PiB and <sup>18</sup>F-florbetapir have been well-investigated in observational studies of AD (9–13). The baseline results from our current study of <sup>11</sup>C-PiB and <sup>18</sup>F-florbetapir PET imaging in the DIAN-TU-001 clinical trial bear out these past findings: at baseline, global cortical SUVR-<sup>11</sup>C-PiB differs statistically significantly from global cortical SUVR-<sup>18</sup>F-florbetapir in both the gantenerumab and placebo arms. After standardizing global cortical SUVR results to the Centiloid scale, global cortical Centiloid-<sup>11</sup>C-PiB shows no statistically significant differences with global cortical Centiloid-<sup>18</sup>F-florbetapir in either arm – a result consistent with the intended purpose of the Centiloid method (14). In the placebo arm only, annualized rates of change did not show statistically significant differences between <sup>11</sup>C-PiB and <sup>18</sup>F-florbetapir, whether measured with SUVR values or standardized to Centiloid units.

However, the effects of anti-Aβ drug treatment on <sup>11</sup>C-PiB and <sup>18</sup>F-florbetapir measures were not compared head-to-head previously. Our results from the gantenerumab arm of the DIAN-TU-001 show that annualized rates of change as measured by global cortical SUVR-<sup>11</sup>C-PiB and global cortical SUVR-<sup>18</sup>F-florbetapir are statistically significantly different, likely due to the greater dynamic range of <sup>11</sup>C-PiB, which appears to result in both greater baseline SUVR values and a greater drug-induced longitudinal decrease in SUVR. After standardizing global cortical SUVR results to the Centiloid scale, global cortical Centiloid-<sup>11</sup>C-PiB shows no statistically significant differences with global cortical Centiloid-<sup>18</sup>F-florbetapir – a result also consistent with the intended purpose of the Centiloid method. Thus, standardizing global cortical Aβ PET biomarker values to the Centiloid scale appears to eliminate statistically significant differences in baseline and longitudinal

measurements made with  $^{11}\text{C}$ -PiB versus  $^{18}\text{F}$ -florbetapir, even when longitudinal changes are modified by anti-A $\beta$  drug treatment as opposed to disease progression alone.

While most previous applications of the Centiloid conversion process have focused on determination of global cortical Centiloids, we also employed the determination of regional Centiloids also described in the original description of the Centiloid process by the direct conversion process (method-2) as described by Klunk and colleagues (14). Here we found that standardizing regional A $\beta$  PET biomarker values to the Centiloid scale appears to eliminate statistically significant differences in longitudinal measurements made with  $^{11}\text{C}$ -PiB versus  $^{18}\text{F}$ -florbetapir in most brain areas.

The brain areas that retain significant differences between regional  $^{11}\text{C}$ -PiB and regional  $^{18}\text{F}$ -florbetapir on the Centiloid scale require further investigation. The change in Centiloids was greater in the  $^{18}\text{F}$ -florbetapir data in the lingual, parahippocampal, and entorhinal cortices – areas which did not show a greater change in the  $^{18}\text{F}$ -florbetapir data when expressed in SUVR units. As these are areas with low retention of both tracers, the signals in these areas are dominated by noise. Thus, this finding may reflect greater noise in the  $^{18}\text{F}$ -florbetapir data. The change in Centiloids was greater in the  $^{11}\text{C}$ -PiB data in subcortical structures such as the caudate and putamen – areas which also showed a greater change in the  $^{11}\text{C}$ -PiB data when expressed in SUVR units. This may relate to the finding that  $^{11}\text{C}$ -PiB shows greater retention in subcortical structures than  $^{18}\text{F}$ -florbetapir in DIAD. For example, in the current dataset, Centiloid- $^{11}\text{C}$ -PiB values at baseline were on average much greater than the global cortical Centiloid- $^{11}\text{C}$ -PiB in the caudate and putamen than Centiloid- $^{18}\text{F}$ -florbetapir values for the same comparisons. Thus, this difference in subcortical change in radiotracer retention may reflect real differences in the tracers and cannot be harmonized by the simple Centiloid conversion. If supported by further study, this will need to be considered in studies where subcortical changes are considered of high importance, such as studies in DIAD and Down syndrome populations where subcortical retention is early and prominent (23–26).

Previously reported annualized reductions of Centiloid- $^{18}\text{F}$ -florbetapir during gantenerumab or other different anti-A $\beta$  monoclonal antibody treatments were greater than those reported in our study (6,7,27,28). This may limit generalizability from DIAD to AD clinical trials. One reason for the discrepancy may be the insufficient amount of drug being administered in the DIAN-TU-001: the initial dose in the DIAN-TU-001 was 225 mg of gantenerumab administered every four weeks, until midway through the trial (approximately two to three years into the trial), when dose escalation was implemented to increase the gantenerumab dose to 1200 mg every four weeks (29). In contrast, the dose escalation in the open-label extension of Marguerite RoAD was implemented over an initial two- to six-month titration period to increase the gantenerumab dose to 1200 mg every four weeks (6). Another contributor could be that individuals with DIAD are generally younger than individuals with late-onset AD and, as one consequence, may have diminished antibody target engagement due to healthier and more intact blood brain barriers (30). Ongoing studies in the gantenerumab DIAN-TU-OLE are testing higher doses due to higher A $\beta$  loads and higher A $\beta$  production (31) in DIAD.

However, reporting only a global cortical Centiloid results in a loss of potential information that can be derived from A $\beta$  PET imaging. Many of the regions showing the largest SUVR/Centiloid differences were subcortical structures and not part of the global cortical SUVR/Centiloid composite used here – although these regions are part of the standard Centiloid cortical volume of interest. It may be informative for future trials to report both global cortical Centiloid – as has traditionally been done – as well as regional Centiloid measures, to reveal the extent to which anti-A $\beta$  drug clearance is a local versus global phenomenon. This may become relevant in addressing the aforementioned question of whether a healthy blood brain barrier is inhibiting anti-A $\beta$  monoclonal antibody penetration throughout the brain. An alternative strategy, which has the potential to be even more informative, would be to transform  $^{18}\text{F}$ -florbetapir PET images into synthetic  $^{11}\text{C}$ -PiB images at the voxel level using an encoding-decoding network (32).

A limitation to this study is that the Centiloid conversion equation for  $^{18}\text{F}$ -florbetapir was established based on a subset of the baseline data of the cohort in this study (33). Therefore, testing for the presence of baseline differences between Centiloid- $^{11}\text{C}$ -PiB and Centiloid- $^{18}\text{F}$ -florbetapir may involve circular reasoning. Additionally, tracer test-retest reliability might have impacted results from the current study; however, previous studies have shown that both  $^{11}\text{C}$ -PiB (34) and  $^{18}\text{F}$ -florbetapir (35) had high test-retest reliability, suggesting that the current results were minimally affected by this phenomenon.

Another limitation to this study is that there is a significant difference in gender balance between the gantenerumab (15 of 41 participants were female, or 37%) and placebo (16 of 25 participants were female, or 64%) arms (Table 2). Differences in gender balance between drug arms may contribute to the statistically significant drug effects seen in the gantenerumab versus placebo comparisons. However, initial findings from the DIANTU-001 also reported statistically significant drug effects in the gantenerumab versus placebo comparisons for  $^{11}\text{C}$ -PiB PET, and in that analysis, baseline demographics were balanced across all drug arms (1). Naturally, this leaves the possibility of differences in gender balance contributing to the statistically significant drug effect seen with  $^{18}\text{F}$ -florbetapir PET; however, a large contribution seems unlikely (36). Nonetheless, future studies are needed to confirm this.

One limitation for future studies is that while Centiloid provides a way for multiple A $\beta$  radiotracers to be used in the same study or trial, the results of our simulated clinical trials suggests that type I error is increased when more than one radiotracer is used. Another challenge for future studies is that while  $^{18}\text{F}$ -florbetapir has been used in the majority of anti-A $\beta$  monoclonal antibody trials in AD that incorporate A $\beta$  PET imaging, using the  $^{11}\text{C}$ -PiB radiotracer offers more power to detect A $\beta$  change in comparison.

Finally, future studies should investigate whether gantenerumab treatment can lead to changes in perfusion to the point of altering A $\beta$  PET SUVR estimates, as  $^{11}\text{C}$ -PiB and  $^{18}\text{F}$ -florbetapir may have different sensitivities to changes in perfusion, which may contribute to the differences observed in annualized rates of SUVR- $^{11}\text{C}$ -PiB and SUVR- $^{18}\text{F}$ -florbetapir change in this study, due to the differences in radiotracer kinetics between  $^{11}\text{C}$ -PiB and SUVR- $^{18}\text{F}$ -florbetapir. Nonetheless, the current study shows that the Centiloid method is

able to harmonize the different annualized rates of SUVR change between  $^{11}\text{C}$ -PiB and  $^{18}\text{F}$ -florbetapir in a clinical trial.

In conclusion, gantenerumab treatment induces longitudinal changes in A $\beta$  PET, and the rates of these longitudinal changes differ significantly between A $\beta$  radiotracers when expressed in SUVR units. These differences were not seen in the placebo arm, suggesting that A $\beta$ -removing treatments pose unique challenges when attempting to compare results across different A $\beta$  radiotracers. Centiloid values derived from PET imaging can harmonize differences between A $\beta$  radiotracers without losing sensitivity to drug effects. Ultimately, until a consensus emerges on how to harmonize drug effects across radiotracers, and since using multiple radiotracers in the same trial may increase type I error, multi-site studies should consider potential variability due to different radiotracers when interpreting A $\beta$  PET biomarker data, and if feasible, use a single radiotracer for the best results.

## Supplementary Material

Refer to Web version on PubMed Central for supplementary material.

## Authors

Charles D. Chen<sup>1</sup>, Austin McCullough<sup>1</sup>, Brian Gordon<sup>1</sup>, Nelly Joseph-Mathurin<sup>1</sup>, Shaney Flores<sup>1</sup>, Nicole S. McKay<sup>1</sup>, Diana A. Hobbs<sup>1</sup>, Russ Hornbeck<sup>1</sup>, Anne M. Fagan<sup>2</sup>, Carlos Cruchaga<sup>3</sup>, Alison M. Goate<sup>4</sup>, Richard J. Perrin<sup>2,5</sup>, Guoqiao Wang<sup>6</sup>, Yan Li<sup>2</sup>, Xinyu Shi<sup>2</sup>, Chengjie Xiong<sup>6</sup>, Michael J. Pontecorvo<sup>7,32</sup>, Gregory Klein<sup>8</sup>, Yi Su<sup>9,10</sup>, William E. Klunk<sup>11</sup>, Clifford Jack<sup>12</sup>, Robert Koeppe<sup>13</sup>, B. Joy Snider<sup>2</sup>, Sarah B. Berman<sup>14</sup>, Erik D. Roberson<sup>15</sup>, Jared Brosch<sup>16</sup>, Ghulam Surti<sup>17</sup>, Ivonne Z. Jiménez-Velázquez<sup>18</sup>, Douglas Galasko<sup>19</sup>, Lawrence S. Honig<sup>20</sup>, William S. Brooks<sup>21</sup>, Roger Clarnette<sup>22</sup>, David Wallon<sup>23</sup>, Bruno Dubois<sup>24,25,26</sup>, Jérémie Pariente<sup>27,28</sup>, Florence Pasquier<sup>29,30</sup>, Raquel Sanchez-Valle<sup>31</sup>, Sergey Shcherbinin<sup>32</sup>, Ixavier Higgins<sup>32</sup>, Ilke Tunali<sup>32</sup>, Colin L. Masters<sup>33</sup>, Christopher H. van Dyck<sup>34</sup>, Mario Masellis<sup>35</sup>, Robin Hsiung<sup>36</sup>, Serge Gauthier<sup>37</sup>, Steve Salloway<sup>38</sup>, David B. Clifford<sup>2</sup>, Susan Mills<sup>2</sup>, Charlene Supnet-Bell<sup>2</sup>, Eric McDade<sup>2</sup>, Randall J. Bateman<sup>2</sup>, Tammie L.S. Benzinger<sup>1</sup>,  
DIAN-TU Study Team

## Affiliations

<sup>1</sup>Mallinckrodt Institute of Radiology, Washington University in St. Louis, St. Louis, MO, USA

<sup>2</sup>Department of Neurology, Washington University in St. Louis, St. Louis, MO, USA

<sup>3</sup>Department of Psychiatry, Washington University in St. Louis, St. Louis, MO, USA

<sup>4</sup>Department of Genetics and Genomic Sciences, Ichan School of Medicine at Mount Sinai, New York, NY, USA

<sup>5</sup>Department of Pathology and Immunology, Washington University in St. Louis, St. Louis, MO, USA

- <sup>6</sup>Department of Biostatistics, Washington University in St. Louis, St. Louis, MO, USA
- <sup>7</sup>Avid Radiopharmaceuticals, Philadelphia, PA, USA
- <sup>8</sup>F. Hoffmann-La Roche Ltd., Basel, Switzerland
- <sup>9</sup>Banner Alzheimer's Institute, Banner Health, Phoenix, AZ, USA
- <sup>10</sup>Arizona Alzheimer's Consortium, Phoenix, AZ, USA
- <sup>11</sup>Department of Psychiatry, University of Pittsburgh, Pittsburgh, PA, USA
- <sup>12</sup>Department of Radiology, Mayo Clinic, Rochester, MN, USA
- <sup>13</sup>Department of Radiology, University of Michigan, Ann Arbor, MI, USA
- <sup>14</sup>Department of Neurology, University of Pittsburgh, Pittsburgh, PA, USA
- <sup>15</sup>Department of Neurology, University of Alabama at Birmingham, Birmingham, Alabama, USA
- <sup>16</sup>Department of Neurology, Indiana University School of Medicine, Indianapolis, IN, USA
- <sup>17</sup>Department of Psychiatry and Human Behavior, Warren Alpert Medical School of Brown University, Providence, RI, USA
- <sup>18</sup>Department of Medicine, University of Puerto Rico School of Medicine, San Juan, PR, USA
- <sup>19</sup>Department of Neurology, University of California San Diego, San Diego, CA, USA
- <sup>20</sup>Department of Neurology, Columbia University, New York, NY, USA
- <sup>21</sup>Prince of Wales Medical Research Institute, University of New South Wales, Sydney, NSW, Australia
- <sup>22</sup>Department of Internal Medicine, University of Western Australia, Crawley, WA, Australia
- <sup>23</sup>Normandie Univ, UNIROUEN, Inserm U1245, CHU Rouen, Department of Neurology and CNR-MAJ, F-76000, Rouen
- <sup>24</sup>Sorbonne Université, AP-HP, GRC n° 21, APM, Hôpital de la Pitié-Salpêtrière, Paris, France
- <sup>25</sup>Institut du Cerveau et de la Moelle Épineière, INSERM U1127, CNRS UMR 7225, Paris, France
- <sup>26</sup>Institut de la Mémoire et de la Maladie d'Alzheimer, Département de Neurologie, Hôpital de la Pitié-Salpêtrière, Paris, France
- <sup>27</sup>Department of Neurology, Hôpital Pierre-Paul Riquet, Centre Hospitalier Universitaire de Toulouse, Toulouse, France
- <sup>28</sup>Toulouse NeuroImaging Centre, Université de Toulouse, Inserm, UPS, France
- <sup>29</sup>Univ. Lille, Inserm, CHU Lille, F-59000 Lille, France

<sup>30</sup>CNR-MAJ, Labex DISTALZ, LiCEND, F-59000 Lille, France

<sup>31</sup>Alzheimer's Disease and Other Cognitive Disorders Unit, Hospital Clínic, Institut d'Investigacions Biomèdiques August Pi i Sunyer (IDIBAPS), Fundació Clínic per a la Recerca Biomèdica, University of Barcelona, Barcelona, Spain

<sup>32</sup>Eli Lilly and Company, Indianapolis, IN, USA

<sup>33</sup>The Florey Institute of Neuroscience and Mental Health, Melbourne, VIC, Australia

<sup>34</sup>Yale School of Medicine, New Haven, CT, USA

<sup>35</sup>Sunnybrook Research Institute, Toronto, ON, Canada

<sup>36</sup>Djavad Mowafaghian Centre for Brain Health, University of British Columbia, Vancouver, BC, Canada

<sup>37</sup>Douglas Mental Health University Institute, Montreal, QC, Canada

<sup>38</sup>Alpert Medical School of Brown University, Providence, RI, USA

## Acknowledgements

We gratefully acknowledge the outstanding commitment of the participants, family members, and caregivers whose participation was critical to the success of the DIAN-TU trial. We thank the DIAN-TU study team for their exceptional dedication and amazing accomplishments which ensured the success of the trial. We appreciate the robust intellectual collaboration between the DIAN-TU investigators, patients and family members, Roche/Genentech, and Eli Lilly & Co., the DIAN-TU Pharma Consortium, the NIH, and regulatory representatives who were critical in making this study possible. We thank the Alzheimer's Association, GHR Foundation, Anonymous Organization, industry partners (Avid Radiopharmaceuticals [a wholly owned subsidiary of Eli Lilly & Co.], Signet, Cogstate), and regulatory representatives for their support.

## Funding

C.D.C. received support from the Knight ADRC T32 fellowship (5T32AG058518-04) and the NSF GRFP (DGE-1745038 and DGE-2139839). N.J.-M. received support from the Alzheimer's Association Research Fellowship (AARFD-20-681815). N.S.M. receives support from the Alzheimer's Association (AARF-21-722022) and BrightFocus Foundation (A2022013F). This study was supported by the Dominantly Inherited Alzheimer Network (DIAN, NIH grants U19AG032438, R01AG052550-01A1), the DIAN Trials Unit (DIAN-TU, NIH grants U01AG042791, U01AG042791-S1, R01AG046179, R01AG53267-S1, as well as support from the Alzheimer's Association, GHR Foundation, an anonymous organization, the DIAN-TU Pharma Consortium, Eli Lilly and Company, Roche, Avid Radiopharmaceuticals, CogState and Bracket), and the Neuroimaging Informatics and Analysis Center (P30NS098577).

## Competing interests

GE Healthcare holds a license agreement with the University of Pittsburgh based on the technology described in this manuscript. Dr. Klunk is a co-inventor of <sup>11</sup>C-PiB and, as such, has a financial interest in this license agreement. GE Healthcare provided no grant support for this study and had no role in the design or interpretation of results or preparation of this manuscript.

Dr. Roberson has been on a DSMB for Lilly and a SAB for AGTC and has received licensing fees from Genentech and owns intellectual property related to tau.

Dr. Holtzman, currently Professor of Neurology, scientific director of the Hope Center for Neurological Disorders, and Associate Director of the Knight ADRC where the research is being conducted, is an inventor on patents for solanezumab, currently being tested in the DIAN-TU clinical trials. If solanezumab is approved as a treatment for Alzheimer's disease or Dominantly Inherited Alzheimer's Disease, Washington University and Dr. Holtzman will receive part of the net sales of solanezumab from Eli Lilly, which has licensed patents related to solanezumab from Washington University.

## Data Availability

Data access to the DIAN–TU trial data will follow the policies of the DIAN–TU data access policy (38), which complies with the guidelines established by the Collaboration for Alzheimer’s Prevention. Patient-related data not included in the paper were generated as part of a clinical trial and may be subject to patient confidentiality. Any data and materials that can be shared will be released via a data/material sharing agreement. Requests to access the DIAN–TU-001 trial data can be made at <https://dian.wustl.edu/our-research/for-investigators/diantu-investigator-resources/>. All code for data cleaning and analysis associated with the current submission is available upon request to the corresponding author and is provided as part of the replication package.

## References

1. Salloway S, Farlow M, McDade E, et al. A trial of gantenerumab or solanezumab in dominantly inherited Alzheimer’s disease. *Nat Med.* June 2021:1–10. [PubMed: 33442018]
2. Liu E, Schmidt ME, Margolin R, et al. Amyloid- $\beta$  11C-PiB-PET imaging results from 2 randomized bapineuzumab phase 3 AD trials. *Neurology.* 2015;85:692–700. [PubMed: 26208959]
3. Landen JW, Andreasen N, Cronenberger CL, et al. Ponezumab in mild-to-moderate Alzheimer’s disease: Randomized phase II PET-PIB study. *Alzheimers Dement (N Y).* 2017;3:393–401. [PubMed: 29067345]
4. Sevigny J, Chiao P, Bussière T, et al. The antibody aducanumab reduces A $\beta$  plaques in Alzheimer’s disease. *Nature.* 2016;537:50–56. [PubMed: 27582220]
5. Mintun MA, Lo AC, Duggan Evans C, et al. Donanemab in Early Alzheimer’s Disease. *New England Journal of Medicine.* 2021;384:1691–1704. [PubMed: 33720637]
6. Klein G, Delmar P, Voyle N, et al. Gantenerumab reduces amyloid- $\beta$  plaques in patients with prodromal to moderate Alzheimer’s disease: a PET substudy interim analysis. *Alzheimer’s Research & Therapy.* 2019;11:101.
7. Swanson CJ, Zhang Y, Dhadda S, et al. A randomized, double-blind, phase 2b proof-of-concept clinical trial in early Alzheimer’s disease with lecanemab, an anti-A $\beta$  protofibril antibody. *Alz Res Therapy.* 2021;13:80.
8. Honig LS, Vellas B, Woodward M, et al. Trial of Solanezumab for Mild Dementia Due to Alzheimer’s Disease. *New England Journal of Medicine.* January 2018.
9. Wolk DA, Zhang Z, Boudhar S, Clark CM, Pontecorvo MJ, Arnold SE. Amyloid imaging in Alzheimer’s disease: comparison of Florbetapir and Pittsburgh Compound-B PET. *J Neurol Neurosurg Psychiatry.* 2012;83:923–926. [PubMed: 22791901]
10. Ni R, Gillberg P-G, Bergfors A, Marutle A, Nordberg A. Amyloid tracers detect multiple binding sites in Alzheimer’s disease brain tissue. *Brain.* 2013;136:2217–2227. [PubMed: 23757761]
11. Su Y, Flores S, Wang G, et al. Comparison of Pittsburgh compound B and florbetapir in cross-sectional and longitudinal studies. *Alzheimer’s & Dementia : Diagnosis, Assessment & Disease Monitoring.* 2019;11:180.
12. Landau SM, Thomas BA, Thurfjell L, et al. Amyloid PET imaging in Alzheimer’s disease: a comparison of three radiotracers. *Eur J Nucl Med Mol Imaging.* 2014;41:1398–1407. [PubMed: 24647577]
13. Thomas BA, Erlandsson K, Modat M, et al. The importance of appropriate partial volume correction for PET quantification in Alzheimer’s disease. *Eur J Nucl Med Mol Imaging.* 2011;38:1104–1119. [PubMed: 21336694]
14. Klunk WE, Koeppe RA, Price JC, et al. The Centiloid Project: standardizing quantitative amyloid plaque estimation by PET. *Alzheimers Dement.* 2015;11:1–15.e1–4. [PubMed: 25443857]
15. Benzinger TLS, Blazey T, Jack CR, et al. Regional variability of imaging biomarkers in autosomal dominant Alzheimer’s disease. *Proc Natl Acad Sci U S A.* 2013;110:E4502–4509. [PubMed: 24194552]

16. Morris JC, Aisen PS, Bateman RJ, et al. Developing an international network for Alzheimer research: The Dominantly Inherited Alzheimer Network. *Clin Investig (Lond)*. 2012;2:975–984.
17. McKay NS, Gordon BA, Hornbeck RC, et al. Neuroimaging within the Dominantly Inherited Alzheimer's Network (DIAN): PET and MRI. *March 2022*:2022.03.25.485799.
18. Su Y, D'Angelo GM, Vlassenko AG, et al. Quantitative Analysis of PiB-PET with FreeSurfer ROIs. *PLOS ONE*. 2013;8:e73377. [PubMed: 24223109]
19. Su Y, Blazey TM, Snyder AZ, et al. Partial volume correction in quantitative amyloid imaging. *Neuroimage*. 2015;107:55–64. [PubMed: 25485714]
20. Fischl B FreeSurfer. *NeuroImage*. 2012;62:774–781. [PubMed: 22248573]
21. Benjamini Y, Hochberg Y. Controlling the False Discovery Rate: A Practical and Powerful Approach to Multiple Testing. *Journal of the Royal Statistical Society: Series B (Methodological)*. 1995;57:289–300.
22. R Core Team. *R: A Language and Environment for Statistical Computing*. Vienna, Austria: R Foundation for Statistical Computing; 2021.
23. Tentolouris-Piperas V, Ryan NS, Thomas DL, Kinnunen KM. Brain imaging evidence of early involvement of subcortical regions in familial and sporadic Alzheimer's disease. *Brain Research*. 2017;1655:23–32. [PubMed: 27847196]
24. Klunk WE, Price JC, Mathis CA, et al. Amyloid Deposition Begins in the Striatum of Presenilin-1 Mutation Carriers from Two Unrelated Pedigrees. *J Neurosci*. 2007;27:6174–6184. [PubMed: 17553989]
25. Chen CD, Joseph-Mathurin N, Sinha N, et al. Comparing amyloid- $\beta$  plaque burden with antemortem PiB PET in autosomal dominant and late-onset Alzheimer disease. *Acta Neuropathol*. 2021;142:689–706. [PubMed: 34319442]
26. Annus T, Wilson LR, Hong YT, et al. The pattern of amyloid accumulation in the brains of adults with Down syndrome. *Alzheimers Dement*. 2016;12:538–545. [PubMed: 26362596]
27. von Rosenstiel P, Gheuens S, Chen T, et al. Aducanumab titration dosing regimen: 24-month analysis from PRIME, a randomized, double-blind, placebo-controlled Phase 1b study in patients with prodromal or mild Alzheimer's disease (S2.003). *Neurology*. 2018;90.
28. Lowe SL, Willis BA, Hawdon A, et al. Donanemab (LY3002813) dose-escalation study in Alzheimer's disease. *Alzheimers Dement (N Y)*. 2021;7:e12112. [PubMed: 33614890]
29. Retout S, Gieschke R, Serafin D, Weber C, Frey N, Hofmann C. Disease Modeling and Model-Based Meta-Analyses to Define a New Direction for a Phase III Program of Gantenerumab in Alzheimer's Disease. *Clinical Pharmacology & Therapeutics*. 2022;111:857–866. [PubMed: 35100444]
30. Sweeney MD, Sagare AP, Zlokovic BV. Blood–brain barrier breakdown in Alzheimer disease and other neurodegenerative disorders. *Nat Rev Neurol*. 2018;14:133–150. [PubMed: 29377008]
31. Potter R, Patterson BW, Elbert DL, et al. Increased in vivo Amyloid- $\beta$ 42 production, exchange, and irreversible loss in Presenilin Mutations Carriers. *Sci Transl Med*. 2013;5:10.1126/scitranslmed.3005615.
32. Shah J, Gao F, Li B, et al. Deep residual inception encoder-decoder network for amyloid PET harmonization. *Alzheimers Dement*. February 2022.
33. Su Y, Flores S, Hornbeck RC, et al. Utilizing the Centiloid scale in cross-sectional and longitudinal PiB PET studies. *Neuroimage Clin*. 2018;19:406–416. [PubMed: 30035025]
34. Tolboom N, Yaqub M, Boellaard R, et al. Test-retest variability of quantitative [11C]PIB studies in Alzheimer's disease. *Eur J Nucl Med Mol Imaging*. 2009;36:1629–1638. [PubMed: 19384547]
35. Joshi AD, Pontecorvo MJ, Clark CM, et al. Performance Characteristics of Amyloid PET with Florbetapir F 18 in Patients with Alzheimer's Disease and Cognitively Normal Subjects. *Journal of Nuclear Medicine*. 2012;53:378–384. [PubMed: 22331215]
36. Johnson KA, Sperling RA, Gidicsin CM, et al. Florbetapir (F18-AV-45) PET to assess amyloid burden in Alzheimer's disease dementia, mild cognitive impairment, and normal aging. *Alzheimer's & Dementia*. 2013;9:S72–S83.
37. Wong DF, Rosenberg PB, Zhou Y, et al. In Vivo Imaging of Amyloid Deposition in Alzheimer Disease Using the Radioligand  $^{18}\text{F}$ -AV-45 (Flobetapir F 18). *J Nucl Med*. 2010;51:913–920. [PubMed: 20501908]



38. Weninger S, Carrillo MC, Dunn B, et al. Collaboration for Alzheimer's Prevention: Principles to guide data and sample sharing in preclinical Alzheimer's disease trials. *Alzheimers Dement.* 2016;12:631–632. [PubMed: 27157073]

Author Manuscript

Author Manuscript

Author Manuscript

Author Manuscript

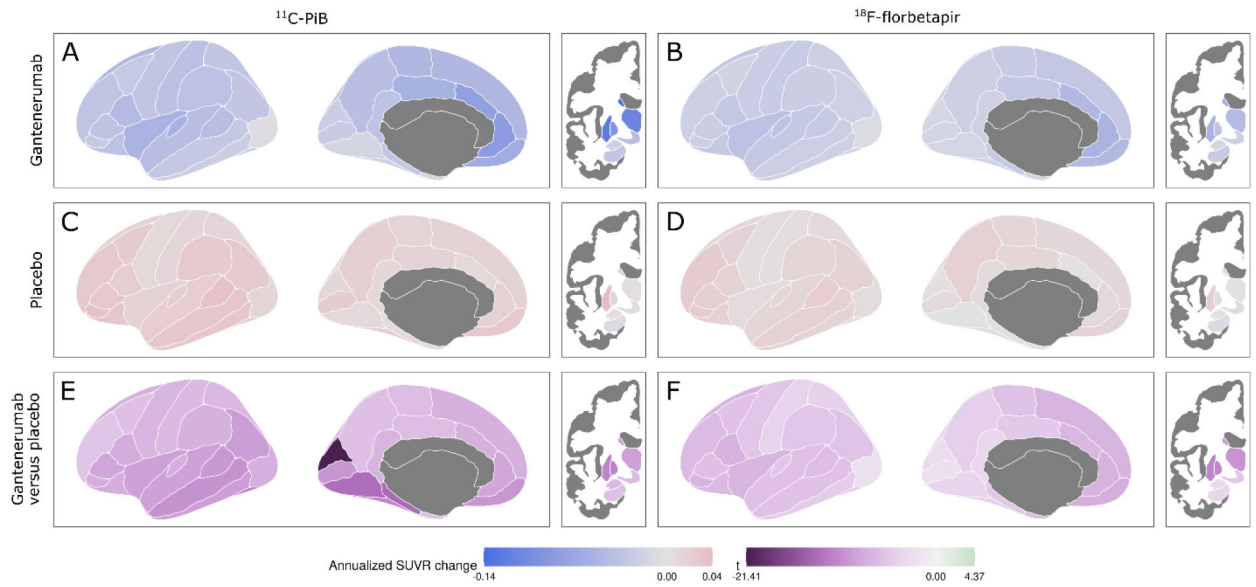


**FIGURE 1.**

Rates of longitudinal change in regional SUVRs. (A, B) Mean annualized SUVR change in the gantenerumab arm as measured by  $^{11}\text{C}$ -PiB and  $^{18}\text{F}$ -florbetapir, respectively. (C, D) Mean annualized SUVR change in the placebo arm as measured by  $^{11}\text{C}$ -PiB and  $^{18}\text{F}$ -florbetapir, respectively. (E, F) Differences between longitudinal change in the gantenerumab arm versus the placebo arm as measured by  $^{11}\text{C}$ -PiB and  $^{18}\text{F}$ -florbetapir, respectively. Only regional comparisons associated with a FDR-adjusted p-value < 0.05 are shown.

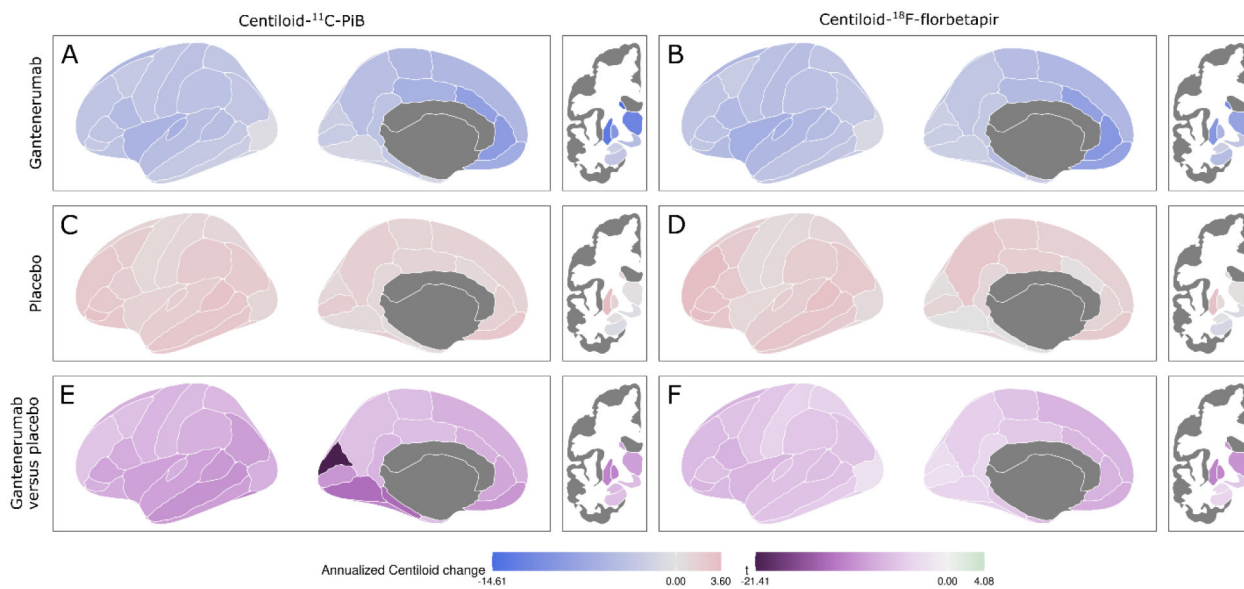


**FIGURE 2.**

Rates of longitudinal change in regional Centiloids. (A, B) Mean annualized Centiloid change in the gantenerumab arm as measured by Centiloid-<sup>11</sup>C-PiB and Centiloid-<sup>18</sup>F-florbetapir, respectively. (C, D) Mean annualized Centiloid change in the placebo arm as measured by Centiloid-<sup>11</sup>C-PiB and Centiloid-<sup>18</sup>F-florbetapir, respectively. (E, F) Differences between longitudinal change in the gantenerumab arm versus the placebo arm as measured by Centiloid-<sup>11</sup>C-PiB and Centiloid-<sup>18</sup>F-florbetapir, respectively. Only regional comparisons associated with a FDR-adjusted p-value < 0.05 are shown.

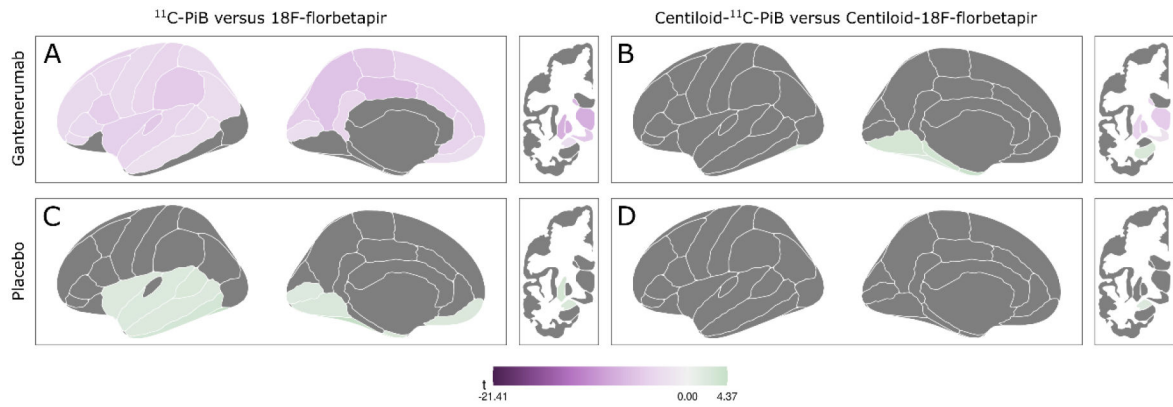


**FIGURE 3.**

Rates of longitudinal change in regional SUVRs versus regional Centiloids. (A) Differences between longitudinal change in the gantenerumab arm as measured by  $^{11}\text{C}$ -PiB versus by  $^{18}\text{F}$ -florbetapir. (B) Differences between longitudinal change in the gantenerumab arm as measured by Centiloid- $^{11}\text{C}$ -PiB versus by Centiloid- $^{18}\text{F}$ -florbetapir. (C) Differences between longitudinal change in the placebo group as measured by  $^{11}\text{C}$ -PiB versus by  $^{18}\text{F}$ -florbetapir. (D) Differences between longitudinal change in the placebo group as measured by Centiloid- $^{11}\text{C}$ -PiB versus by Centiloid- $^{18}\text{F}$ -florbetapir. Only regional comparisons associated with a FDR-adjusted p-value  $< 0.05$  are shown.

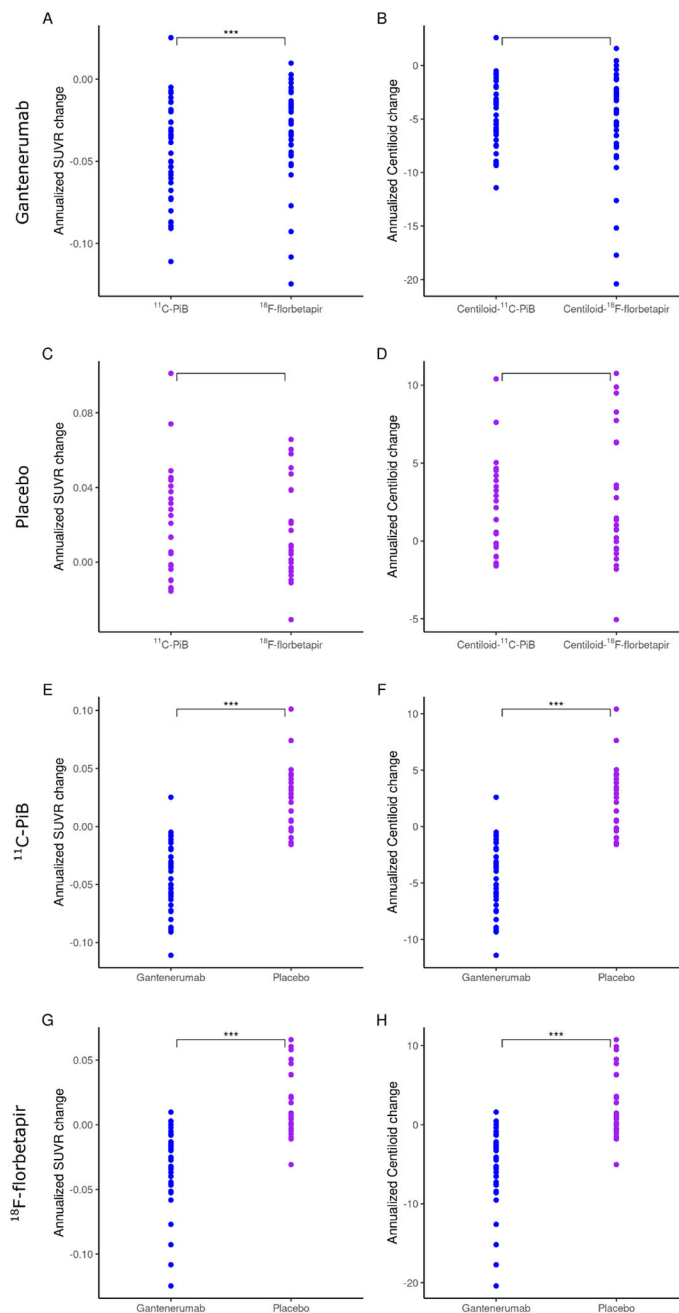


**FIGURE 4.**

Rates of longitudinal change in global cortical SUVRs and Centiloids. (A) Annualized SUVR change in the gantenerumab arm as measured by  $^{11}\text{C}$ -PiB and  $^{18}\text{F}$ -florbetapir. (B) Annualized Centiloid change in the gantenerumab arm as measured by Centiloid- $^{11}\text{C}$ -PiB and Centiloid- $^{18}\text{F}$ -florbetapir. (C) Annualized SUVR change in the placebo arm as measured by  $^{11}\text{C}$ -PiB and  $^{18}\text{F}$ -florbetapir. (D) Annualized Centiloid change in the placebo arm as measured by Centiloid- $^{11}\text{C}$ -PiB and Centiloid- $^{18}\text{F}$ -florbetapir. (E) Annualized SUVR change in the gantenerumab and placebo arms as measured by  $^{11}\text{C}$ -PiB. (F) Annualized Centiloid change in the gantenerumab and placebo arms as measured by Centiloid- $^{11}\text{C}$ -PiB.

(G) Annualized SUVR change in the gantenerumab and placebo arms as measured by  $^{18}\text{F}$ -florbetapir. (H) Annualized Centiloid change in the gantenerumab and placebo arms as measured by Centiloid- $^{18}\text{F}$ -florbetapir. \*p-value<0.05, \*\*p-value<0.01, \*\*\*p-value<0.001.

Author Manuscript

Author Manuscript

Author Manuscript

Author Manuscript

TABLE 1

A $\beta$  PET radiotracers used in Phase 2 and Phase 3 clinical trials of anti-A $\beta$  monoclonal antibodies for AD

Anti-A $\beta$ monoclonal antibody	Sponsor	Clinical trial	A $\beta$ PET radiotracer
<b>Aducanumab</b>	Biogen	<a href="#">NCT02477800</a> <a href="#">NCT02484547</a>	<sup>18</sup> F-florbetapir
<b>Bapinezumab</b>	Janssen and Pfizer	<a href="#">NCT00574132</a> <a href="#">NCT00575055</a> <a href="#">NCT00667810</a> <a href="#">NCT00676143</a> <a href="#">NCT00996918</a> <a href="#">NCT00998764</a>	<sup>11</sup> C-PiB
<b>Crenezumab</b>	Roche	<a href="#">NCT02670083</a>	<sup>18</sup> F-florbetapir
<b>Donanemab</b>	Eli Lilly	<a href="#">NCT03367403</a>	<sup>18</sup> F-florbetapir
<b>Gantenerumab</b>	Roche and Washington University School of Medicine *	<a href="#">NCT01224106</a> <a href="#">NCT01760005</a> * <a href="#">NCT02051608</a> <a href="#">NCT03443973</a> <a href="#">NCT03444870</a> <a href="#">NCT03444870</a>	Florbetaben, <sup>18</sup> F-florbetapir, flutemetamol, and <sup>11</sup> C-PiB
<b>Lecanemab</b>	Eisai	<a href="#">NCT03887455</a>	<sup>18</sup> F-florbetapir
<b>Ponezumab</b>	Pfizer	<a href="#">NCT00945672</a>	<sup>11</sup> C-PiB
<b>Solanezumab</b>	Eli Lilly and Washington University School of Medicine *	<a href="#">NCT01127633</a> <a href="#">NCT01760005</a> * <a href="#">NCT01900665</a> <a href="#">NCT02008357</a> <a href="#">NCT02760602</a>	<sup>18</sup> F-florbetapir and <sup>11</sup> C-PiB

Information on clinical trials was accessed from [alzforum.org](#), [clinicaltrials.gov](#), and [accessdata.fda.gov](#) on 2021-06-25.

\* Washington University School of Medicine was the sponsor for this trial. To our knowledge, no other clinical trial in AD has performed a head-to-head comparison of two A $\beta$  radiotracers.

TABLE 2

## Participant characteristics

		Gantenerumab	Placebo
<b>Number</b>		41	25
<b>Female, n</b>		15 (37%)	16 (64%)
<b>Mean age (SD)</b>		46 (10)	44 (10)
<b>CDR<sup>®</sup>, n</b>	<b>=0</b>	25 (61%)	14 (56%)
	<b>&gt;0</b>	16 (39%)	11 (44%)
<b>Mean EYO (min, max)</b>		-2.1 (-14, 10)	-2.4 (-15, 10)
<b>Family mutation, n</b>	<b>PSENI</b>	34 (83%)	18 (72%)
	<b>PSEN2</b>	3 (7%)	2 (8%)
	<b>APP</b>	4 (10%)	5 (20%)
<b>APOE, n</b>	<b>e4-</b>	29 (71%)	17 (68%)
	<b>e4+</b>	12 (29%)	8 (32%)

Abbreviations: *APOE* (apolipoprotein E), *APP* (A $\beta$  precursor protein), CDR<sup>®</sup> (Clinical Dementia Rating<sup>®</sup>), EYO (Estimated Years to symptom Onset), *PSENI* (presenilin-1), *PSEN2* (presenilin-2), SD (standard deviation).

Author Manuscript

Author Manuscript

Author Manuscript

Author Manuscript



**TABLE 3**

Mean baseline global cortical SUVR and Centiloid in the gantenerumab and placebo arms as measured by <sup>11</sup>C-PiB and <sup>18</sup>F-florbetapir

	Gantenerumab	Placebo	Gantenerumab versus placebo t-value (p-value)	Gantenerumab versus placebo Cohen's d [95% CI]
Mean baseline global cortical SUVR- <sup>11</sup> C-PiB [95% CI]	1.7 [1.5, 1.9]	1.7 [1.5, 1.9]	0.34 (0.74)	0.08 [-0.40, 0.57]
Mean baseline global cortical SUVR- <sup>18</sup> F-florbetapir [95% CI]	1.5 [1.4, 1.6]	1.4 [1.3, 1.5]	0.72 (0.48)	0.18 [-0.31, 0.66]
Global cortical SUVR- <sup>11</sup> C-PiB versus SUVR- <sup>18</sup> F-florbetapir t-value (p-value)	5.5 ( $2.7 \times 10^{-6}$ ) <sup>***</sup>	4.2 (0.00030) <sup>***</sup>		
Global cortical SUVR- <sup>11</sup> C-PiB versus SUVR- <sup>18</sup> F-florbetapir Cohen's d	0.85 [0.49, 1.21]	0.84 [0.38, 1.30]		
Mean baseline global cortical Centiloid- <sup>11</sup> C-PiB [95% CI]	63 [46, 80]	59 [41, 77]	0.34 (0.74)	0.08 [-0.40, 0.57]
Mean baseline global cortical Centiloid- <sup>18</sup> F-florbetapir [95% CI]	61 [43, 79]	52 [35, 69]	0.72 (0.48)	0.18 [-0.31, 0.66]
Global cortical Centiloid- <sup>11</sup> C-PiB versus Centiloid- <sup>18</sup> F-florbetapir t-value (p-value)	0.43 (0.67)	1.17 (0.25)		
Global cortical Centiloid- <sup>11</sup> C-PiB versus Centiloid- <sup>18</sup> F-florbetapir Cohen's d [95% CI]	0.07 [-0.24, 0.37]	0.23 [-0.17, 0.63]		

\* p-value<0.05,

\*\* p-value<0.01,

\*\*\* p-value<0.001.

Abbreviations: CI (confidence interval), SD (standard deviation).

TABLE 4

Mean rates of longitudinal change in global cortical SUVR and Centiloid in the gantenerumab and placebo arms as measured by  $^{11}\text{C}$ -PiB and  $^{18}\text{F}$ -florbetapir

	Gantenerumab	Placebo	Gantenerumab versus placebo t-value (p-value)	Gantenerumab versus placebo Cohen's d [95% CI]
Mean annualized global cortical SUVR- $^{11}\text{C}$ -PiB change (SE)	-0.045 (0.009)	0.022 (0.008)	-8.9 ( $6.6 \times 10^{-12}$ ) ***	-2.24 [-2.90, -1.58]
Mean annualized global cortical SUVR- $^{18}\text{F}$ -florbetapir change (SE)	-0.030 (0.008)	0.015 (0.009)	-6.6 ( $1.7 \times 10^{-8}$ ) ***	-1.64 [-2.21, -1.06]
Global cortical SUVR- $^{11}\text{C}$ -PiB change versus SUVR- $^{18}\text{F}$ -florbetapir change t-value (p-value)	-3.9 (0.00034) ***	1.2 (0.26)		
Global cortical SUVR- $^{11}\text{C}$ -PiB change versus SUVR- $^{18}\text{F}$ -florbetapir change Cohen's d [95% CI]	-0.61 [-0.94, -0.27]	0.23 [-0.17, 0.63]		
Mean annualized global cortical Centiloid- $^{11}\text{C}$ -PiB change (SE)	-4.6 (0.9)	2.2 (0.8)	-8.9 ( $6.6 \times 10^{-12}$ ) ***	-2.24 [-2.90, -1.58]
Mean annualized global cortical Centiloid- $^{18}\text{F}$ -florbetapir change (SE)	-5 (1)	3 (2)	-6.6 ( $1.7 \times 10^{-8}$ ) ***	-1.64 [-2.21, -1.06]
Global cortical Centiloid- $^{11}\text{C}$ -PiB change versus Centiloid- $^{18}\text{F}$ -florbetapir change t-value (p-value)	0.62 (0.54)	-0.38 (0.71)		
Global cortical Centiloid- $^{11}\text{C}$ -PiB change versus Centiloid- $^{18}\text{F}$ -florbetapir change Cohen's d [95% CI]	0.10 [-0.21, 0.40]	-0.08 [-0.47, 0.32]		

\* p-value<0.05,

\*\* p-value<0.01,

\*\*\* p-value<0.001.

Abbreviations: CI (confidence interval), SE (standard error).

**TABLE 5**

Type I error and power (%) comparison when using both Centiloid-<sup>11</sup>C-PiB and Centiloid-<sup>18</sup>F-florbetapir in 1000 simulated clinical trials

	No treatment effect (type I error comparison)					With observed treatment effect (power comparison)				
Percent (%) of participants scanned with <sup>18</sup> F-florbetapir	100	75	50	25	0	100	75	50	25	0
<b>20 participants per arm</b>	4.8	9.3	14.8	9.7	4.3	52.9	63.3	65.0	72.5	84.3
<b>32 participants per arm</b>	4.9	8.2	14.6	9.4	5.7	74.4	81.1	83.7	88.4	98.0
<b>40 participants per arm</b>	4.5	8.0	15.0	9.6	4.9	85.0	88.2	88.6	93.9	98.9
<b>With 5% annual dropout</b>										
<b>20 participants per arm</b>	4.6	9.8	12.2	8.5	4.1	48.7	54.8	60.7	67.2	76.5
<b>32 participants per arm</b>	6.0	8.6	13.6	9.9	5.7	67.8	73.1	76.6	84.9	92.1
<b>40 participants per arm</b>	4.7	8.0	11.9	9.4	5.0	78.5	82.2	85.5	94.4	97.6

Each simulated dataset was analyzed using linear mixed models and the treatment effect was defined as the difference between the slopes (annual rate of change in Centiloid). Two-sided t-tests were used with a nominal type I error of 5%.